International Journal of Applied Engineering Research ISSN 0973-4562 Volume 12, Number 23 (2017) pp. 13064-13076

Ultra-High-Strength Grout for Filling Steel Pipes in Offshore Wind Turbines

MyungKwan Lim[1] and SangSu Ha [2, *]

[1]Assistant professor, Dr., Dept. Of Architectural Engineering, Songwon University, Gwangju Metropolitan City, Republic of Korea.

[2]Associate professor, Division of Real Estate and Construction Engineering (Major in Urban Planning and Architecture Engineering), 40(16979): 40, Gangnam-ro, Giheung-gu, Yongin-si, Gyeonggi-do, 16979, Korea.

** Corresponding Author*
Orcid: 0000-0002-0493-4439 & IDsScopus Author ID: 57192715396

Abstract

In South Korea, the national energy master plan for the period from 2003 to 2030 aims to obtain nearly 11% of the total energy production from offshore wind power generation. Offshore wind turbines are similar to wind turbines installed on the ground, except for the fact that the lower portion of the wind turbine is submerged in seawater, and grout is filled in the transition piece that connects the upper portion of the turbine to the lower portion. Therefore, the mechanical properties and durability characteristics of the grout used in the turbine are important for the prevention of damage to the transition piece caused by seawater. The process for deriving a balanced mixing ratio to develop ultra-high-strength grout for offshore wind turbines is described in this study. Based on the derived final mixing ratio, the mechanical properties and durability characteristics of the grout were investigated. It was predicted that the use of high-speed hardening calcium sulfo-aluminate admixture (HSH-CSA) and anhydrous gypsum for securing early strength would interfere with the long-term strength of the turbine. The final mixture of HSH-CSA and anhydrous gypsum (25%), silica fume (6.5%), and silica sand (40%) was derived for the development of 100-MPa-class ultra-high-strength grout for offshore wind turbines, which was the target of this study.

Keywords: Offshore wind power generator, Anhydrous gypsum, High speed hardening Calcium- , Sulfo-aluminate Admixture

INTRODUCTION

With the recent development of offshore wind turbines, there is a growing interest in their supporting areas. In particular, more than 70% of offshore wind turbines use monopiles as a support and grout is injected into the transition piece that connects the monopile and the tower. According to a recent Scottish & Southern Energy report [1], there was a loss of nearly GBP 25 million in the UK alone due to the usage of defective grout in offshore wind turbines. This data corresponded to 600 wind turbines installed in 13 wind farms, and it indicates that the quality of grout plays an important role in offshore wind power generation. The monopiles for offshore wind turbines are manufactured at factories and transported to the sites for assembly.

The construction of the monopile transition piece includes the processes of mounting the upper portion of the turbine on the transition piece located at the top of the lower portion using a hydraulic jack, fixing it with bolts, filling grout between the lower portion and the transition piece, and sealing the transition piece with rubber [2,3]. The quality of grout used and the construction technology are critical factors because the lower portion of the wind turbine is immersed in seawater, which can interfere with the smooth construction of the turbine and cause damage to the transition piece filled with grout. However, because the mechanical properties and durability of the grout generally used in civil engineering and construction in South Korea is significantly low compared to overseas products, it is urgently required to develop advanced technologies [4,5] for the manufacture of high-strength grout for use in offshore wind turbines.

In general, during the installation of a 2-MW offshore wind turbine, approximately 300 t of the turbine weight and an additional 120 t of the upper portion weight are transferred to the transition piece as load. Therefore, offshore wind turbines need to use grout having a compressive strength above 100-MPa, which is remarkably superior in quality to the conventional grout with a compressive strength of 35 MPa. Furthermore, the grout used in wind turbines must have excellent resistance to mechanical properties such as fatigue load [6].

Because standards for the mechanical properties and volume relating to grout are prone to changes and regulations for its durability are not established, it is virtually impossible to apply grout that is suitable to offshore wind turbines as per Korean standards. The purpose of this study is to develop an ultra-high-strength grout for offshore wind turbines, which has high early strength compared to the conventional grout.

MATERIALS USED AND EXPERIMENTAL METHODS

Materials used

The ultra-high-strength grout developed in this study for offshore wind turbines has excellent early-age strength, fatigue strength, and resistance to fracture as well as excellent workability.

Table 1 shows the target performance of the ultra-high-strength grout developed in this study.

Table 1: Target performance of the ultra-high-strength grout for offshore wind turbines

Evaluation factor	Unit	Benchmark level (country/company)	Development target	Evaluation method
Workability	-	Excellent (Densit, Denmark)	Excellent	-
Density	kN/m3	20 (Densit, Denmark)	Over 20 (28 days of age)	KS M 0602
Compressive strength	MPa	130 (BASF, Germany)	Over 100 (28 days of age)	KS F 4042
Elastic modulus	GPa	55 (Densit, Denmark)	Over 40 (28 days of age)	KS F 4042
Early strength (within 24 h)	MPa	60 (Densit, Denmark)	Over 30 (1 day of age)	KS F 4042
Flexural strength	MPa	18 (Densit, Denmark)	Over 10 (28 days of age)	KS F 4042
Bond strength	MPa	-	Over 100% compared to the highest specification (28 days of age)	KS F 4042
Pullout strength	MPa	-		ACI 352.2-04
Autogenous shrinkage	10-6	0 (BASF, Germany)	Below 300 (28 days of age)	KS F 2586
Carbonation	mm/week	-	Over 100% compared to the highest specification (28 days of age)	KS F 2584
Freeze-thaw	DF	-		ASTM C 666 KS F 2456
Chemical resistance	wt(%)	-		ASTM C 267, 579

An excellent grout must have a compressive strength of over 100 MPa, an elastic modulus of over 40 GPa, an early strength within 24 h that reaches approximately 30% of the strength at 28 days of age, and a flexural strength of over 10 MPa. It must have excellent durability against wind, sea waves, and vibration generated by turbine rotation, as well as excellent fatigue strength and resistance to fracture.

In order to develop the ultra-high-strength grout with a compressive strength of over 100 MPa, a proper mix was selected after more than ten trials performed over four months. The compressive strength up to 28 days was estimated using a mix that showed a compressive strength of about 30 MPa at three days of age.

Tables 2, 3, 4, and 5 show the physical and chemical properties of the major materials used for developing the grout. Silica sand with a 5-mm particle size was used as fine aggregate and HSH-CSA was used as cement. Anhydrous gypsum was added to the mix. As the ratio of HSH-CSA to anhydrous gypsum is closely related to ettringite generation, using an appropriate ratio may increase the early strength due to the hydration promoting effect. Failure to use an appropriate ratio may cause severe cracking by inducing rapid expansion of the grout [7]. Therefore, an appropriate mixing range was determined through experimental mixing. Extremely fine silica fume was added to improve the strength, and a retarding agent, antifoaming agent, and superplasticizer were used to ensure workability.

Table 2: Physical & chemical properties of high-speed hardening CSA (HSH-CSA)

Physical Properties		Chemical composition (%)						
Density (g/cm^3)	Specific surface area (cm^2/g)	SiO_2	Al_2O3	Fe_2O_3	CaO	MgO	SO_3	F-CaO
2.9	≤2,000	1	8	0.5	50	2	27	16

Table 3: Physical & chemical properties of anhydrous gypsum

Physical Properties		Chemical composition (wt%)				
Colors	Shape	Chemical water	SO_3	CaO	$CaSO_4$	CaF_2
2.9	≤2,000	0.5	2	8	90	3

Table 4: Physical & chemical properties of the Silica Fume (SF)

Chemical composition						
Density (g/cm^3)	Loss ignition (%)	Fineness (cm^2/g)	Shape	Grain size (μm)	Weight of unit volume (kg/m^3)	Main ingredient
2.2	3.45	Approximately 280,000	Rectangle	1	278	Silicon

Chemical composition (%)					
SiO_2	Al_2O_3	Al_2O_3	CaO	MgO	SO_3
85	1.5	3.0	0.7	2.0	0.2

Table 5: Physical & chemical properties of the blast furnace slag (BFS)

Chemical composition

Type		Density (g/cm^3)	Average particle size (μm)	Residue (45μm, %)	Specific surface area (cm^2/g)	Moisture (%)
Blast Furnace slag	Type 1	2.82	3	-	8,200	0.4
	Type 2		6	-	6,800	
	Type 3		11	2.0	4,300	

Chemical composition (%)						
SiO_2	Al_2O_3	Fe_2O_3	CaO	MgO	SO_3	Loss on ignition
34.0	14.0	0.4	443.0	5.5	2.5	3.3

Experimental methods

In this study, in order to develop grout for offshore wind turbines, basic experiments for judging the suitability of grout as a filling material inside the wind turbine were conducted in Stage 1.

In Step 1, compressive strength, elastic modulus, and flexural strength tests were conducted as basic experiments to develop the core mixture and to compare it with the conventional grout products. Each experiment was conducted in accordance with Korean Standard (KS) and five specimens were produced according to the experimental condition and measurement date. The experimental results were obtained by arithmetically averaging the three experimental measurements except the highest and lowest measurements.

In Step 2, a series of experiments for the workability, density, strength characteristics, and durability characteristics were conducted to determine the suitability of the final mix as a filling material. In addition, the utilization suitability of the developed grout (developed grout product, hereafter called

"D.G.P") was evaluated by comparing each property with that of the highest grade grout sold by company A in South Korea (commercial grout product, hereafter called "C.G.P").

Determination of workability and density

After grouting, a flow test was conducted in accordance with **KS F 2476 [**7]. The specimen was cut into 40×40×40 mm samples using a cutting machine in accordance with **KS M 0602 [**8] and the density was calculated using the measured dry mass and volume of the specimen in the surface-dry condition.

Determination of strength properties (compressive strength, early strength, elastic modulus, flexural strength, bond strength, and pullout strength)

Following grouting, samples of 40×40×160 mm size were prepared in accordance with **KS F 4042** [9]. After demolding and underwater curing (20 ℃), the compressive strength was measured at 1, 3, 7, 28, and 56 days of age. The early strength was set as the compressive strength at 1 day of age. The elastic modulus was estimated by equation (1) using the compressive strength, and the flexural strength was calculated by equation (2) using the central point loading method with 40×40×160 mm samples.

$$E_c = 8500\sqrt[3]{f_{ck}}\ , \qquad \text{Equation (1)}$$

$$R_f = 3F_f L/2bh^2, \qquad \text{Equation (2)}$$

where E_c represents the elastic modulus (Gpa), f_{ck} the compressive strength at 28 days of age (MPa), R_f the flexural strength (MPa), b the width of the specimen (mm), h the thickness of the specimen (mm), F_f the maximum load (N), and L the distance between the supports (mm).

For the measurement of the bond strength, the prepared specimens underwent two-day wet curing (20±3 ℃ and relative humidity of 90% or higher) after grouting in accordance with the standard method. The specimens were then demolded, submerged in water up to 15 mm height, and cured at 20±3 ℃ temperature and 60±10% relative humidity for 26 days.

After curing, a 40×40 mm bond strength attachment was fixed to the specimen using a two-component epoxy resin. After 24 h, tensile stress with a 2000 N/min loading rate was applied in the vertical direction to obtain the bond strength. As shown in Figure 1, a D16 reinforcing bar was placed at the center of a 250×250×200 mm rectangular parallel pipe to measure the pullout strength.

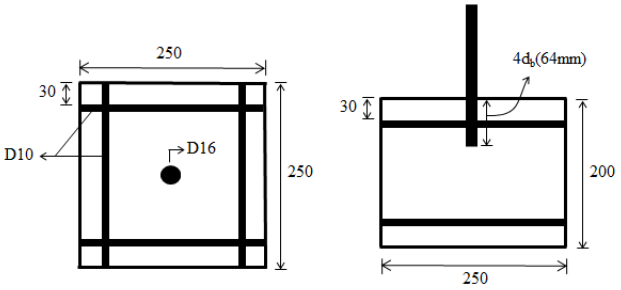

(a) Placement and shape of the reinforcing bar in the specimen

(b) Pullout strength experimental setup

Figure 1: Pullout strength experimental setup (ACI 352.2-04)

The buried length of the reinforcing bar was 64 mm, which was four times the diameter of the bar, and the pullout strength was measured using a universal testing machine.

Determination of durability properties (autogenous shrinkage, carbonation, freeze-thaw, and chemical resistance)

To determine the autogenous shrinkage, a Teflon sheet was applied to the inside of the specimen to prevent moisture from escaping due to restrictions or drying. The specimen was demolded at day 1 of age and the entire surface was sealed with aluminum tape before measurement. The first measurement of the autogenous shrinkage of the grout was conducted after the initial setting of the grout.

The carbonation experiment was conducted in accordance with **KS F 2584** [10]. The experimental conditions were 20±2 ℃ temperature, 60±5% humidity, and 5±0.2% CO_2 concentration. The freeze-thaw experiment was conducted under a freezing temperature of −18 ℃ and a melting temperature of 5 ℃ in accordance with **ASTM C 666 [**11] Procedure B (rapid freezing and thawing). The relative dynamic modulus of elasticity by the first resonance frequency was evaluated after 100 cycles, where one cycle represented three hours.

For the chemical resistance experiment, a cylindrical specimen with 100-mm diameter and 200-mm height was used in accordance with **ASTM C 267, 579 [**12–13]. After

demolding within 48 h, the specimen was cured in water for 28 days at 20±2 ℃ temperature. In order to measure its resistance to acid, samples of the specimen were immersed in 5% solutions of hydrochloric acid, sulfuric acid, and nitric acid and the mass change rate was measured at 1, 2, 4, and 8 weeks of age. The mass change rate was calculated using equation (3).

Mass change rate (%) = $\frac{W_n - W_o}{W_n}$, Equation (3)

where W_n : mass of the specimen after immersion for the specified period

W_o : mass of the specimen before immersion.

MIX DESIGN AND EXPERIMENTAL PROCESS

In order to apply grout to offshore wind turbines, it is necessary to develop the related technologies. The high-performance grout produced in South Korea has a compressive strength of up to 70 MPa, which is far below the performance level required for use in offshore wind turbines. The following experiment was conducted as a basic step to develop high-performance grout for offshore wind turbines, which has higher strength and durability than the grout sold in the Korean market.

In order to find the optimal mixing ratio to reach the target grout strength, mixtures were prepared using various binders and admixtures. Mixing was performed in four steps. In each step, the mixing ratio was adjusted within the range of each material. After mixing, measurements were taken for the flow, compressive strength, elastic modulus, and flexural strength among others and the results were displayed.

The mixtures in each step were composed of the main ingredients, fine aggregate, and function-improving additives as shown in **Table 6**. Cement and blast furnace slag, which are binders, were used as the main ingredients and silica sand with a 5-mm particle size was used as the fine aggregate. Superplasticizer, HSH-CSA, and antifoaming agent were used as function-improving additives.

Stage 1 (Step 1) mix design

The conventional grout from company S in South Korea and the grout from the preliminary experiment shown in **Table 6** were evaluated based on their compressive strengths alone. Experimental results of the developed samples showed that the early strength, i.e., the strength at 1 day of age, was low and the strength at 28 days could not reach 100 MPa. The conventional grout showed high early strength at 1 day of age but low strength at 28 days of age.

Table 6: Basic mix design

Main ingredient	Fine aggregate	+ Enhanced additive
Cement+BFS	Max Size 5 mm	Superplasticizer, high-speed hardening CSA, Air-detraining admixture

Therefore, in order to increase the compressive strength at 28 days, which is the design strength, the amount of cement was increased and the fine powder of silica fume and blast furnace slag were mixed as shown in **Table 7**. The specific mixing ratios for each material were provided to examine their influence on the strength.

Stage 1 (Step 2) mix design

In this mix, HSH-CSA and anhydrous gypsum were used instead of the cement binder in Step 1 to improve the early strength. It has been reported that HSH-CSA and anhydrous gypsum initially produce large amounts of ettringite, thereby improving the early strength [14,15,16]. However, their use in large amounts may cause the rapid expansion of grout and generate severe cracking, because of which their quantities were restricted.

Table 8 shows the mixing ratios of Step 2. The specific mixing ratios for each material were provided to examine their influences on the strength.

Stage 1 (Step 3) mix design

In order to achieve higher early strength than Step 2 and increase the long-term strength, the proportions of HSH-CSA and anhydrous gypsum were adjusted and silica fume was added. As the proportions of HSH-CSA and anhydrous gypsum are closely related to ettringite generation, they have a predominant effect on the early strength as well as the long-term strength.

Table 7: Mix design for high-strength grouting

Grout	Cement (%)	Expansive admixture (%)	BFS (%)	Silica (%)	Air-detraining admixture (%)	Superplasticizer (%)	Water (%)
Step 1	43	4	6.5	25	1	1	15.8
Note: Increasing the amount of cement							

Table 8: Advanced mix design of high strength grouting

Grout	HSH-CSA (%)	Anhydrous gypsum (%)	Silica fume (%)	Silica (%)	Air-detraining admixture (%)	Superplasticizer (%)	Water (%)
Step 2	30	6.5	-	25	0.5	1.5	16.5
Step 3	25	25	6	40	0.5	1.5	16.5
Step 4	25	25	25	40	0.5	1.5	16.5

Note: Step 1. Adjust the amount of HSH-CSA & Anhydrous gypsum to promote long-term strength & early strength
Step 2. Adjust the amount of HSH-CSA & Anhydrous gypsum to promote long-term strength & early strength

Table 9: Optimal mix design (Stage 2)

Grout	HSH-CSA (%)	Anhydrous gypsum (%)	Silica fume (%)	Silica (%)	Air-detraining admixture (%)	Superplasticizer (%)	Water (%)
Final	25	25	6.5	40	0.5	1.5	16.5

Silica fume is a widely used admixture for strength improvement. It is currently widely used for the manufacture of high-strength and high-durability grout. **Table 8** shows the mixing ratio required to achieve higher long-term strength than Step 2. The specific mixing ratios for each material were provided to examine their influences on the strength.

Stage 1 (Step 4) mix design

In order to achieve higher early strength and long-term strength than Step 3, ultra-high-speed hardening cement was used. Furthermore, the proportions of HSH-CSA and anhydrous gypsum were slightly adjusted and the proportion of silica fume was increased to improve the long-term strength.

Table 8 shows the mixing ratio required to achieve higher strength than Step 3. The specific mixing ratios for each material are provided to examine their influences on the strength.

Stage 2 mix design

As shown in Table 9, the optimal mixing condition was determined based on the mix selected in Step 4. The utilization and suitability of the grout developed for wind turbines were evaluated through comparison with the C.G.P. The measurement factors, compressive strength, and workability were measured in the same manner as in the previous stage. Furthermore, the mechanical properties were examined by comparing the flexural strength and the elastic modulus.

EXPERIMENT RESULTS AND DISCUSSION

Stage 1-experiment results

As shown in **Figure 2**, early strength (compressive strength at 1 day of age) in Step 1 could not be measured because the grout had not hardened. The compressive strength was 30–50 MPa at 3 days of age, 40-60 MPa at 7 days of age, and 70-80 MPa at 28 days of age. The strength at 28 days was approximately 10-MPa higher than that of the conventional grout, but the early strength was significantly lower. The flexural strength was within 10% of the compressive strength at 3, 7, and 28 days of age.

According to the KS, in terms of workability, the flow value of grout is specified at 220 mm or more, but it was 90–110 mm in the D.G.P, which was significantly lower than the standard value. The fluidity of the grout is important because pumps are used for the grouting process; therefore, it is required to increase the grout fluidity to improve the construction performance.

The experiment in Step 2 showed that the early strength (at 1 day of age) was 10–30 MPa, indicating significantly improved early strength compared to the case where only regular cement was used. The compressive strength was 40–50 MPa at 3 days of age, 40–60 MPa at 7 days, and 60–80 MPa at 28 days. The early strength was increased compared to Step 1 due to an early increase in ettringite production, but the strength at 28 days was decreased. This is because the initial increase in the hydration led to increased expansion, thereby resulting in slightly more micro-cracks in the inner transition zone.

Although the flow value obtained in Step 1 was below the standard level, it increased to more than 220 mm in Step 2 because of increasing the amount of superplasticizer, and thus met the standard value.

Figure 3 shows the compressive strength test results. The compressive strength test (KS L ISO 679) results of Step 3 in **Figure 4** show that the early strength (at 1 day of age) was 20–40 MPa, which was slightly higher compared to Step 2. The compressive strength was 30–50 MPa at 3 days, 50–60 MPa at 7 days, and 70–90 MPa at 28 days. The strength at 28 days was also slightly higher.

The compressive strength test results of Step 4 revealed that the early strength was not significantly different from that of Step 3 because the early strength (at 1 day of age) was 20–40 MPa and the strength at 3 days was 30–50 MPa. However, the strength was 70–90 MPa at 7 days and 90–100 MPa at 28 days. The strength at 28 days was higher than that of Step 3. This is because, unlike Step 2, the substitution of silica fume increased the fineness and hydration reaction, thereby resulting in more dense internal structure. Step 4 yielded the results that correspond to the targeted properties of this study.

In this study, the physical properties of the final mix were compared with those of the conventional C.G.P. **Figures 5 and 6** show the compressive strength test results of Step 4 and of all the steps, respectively.

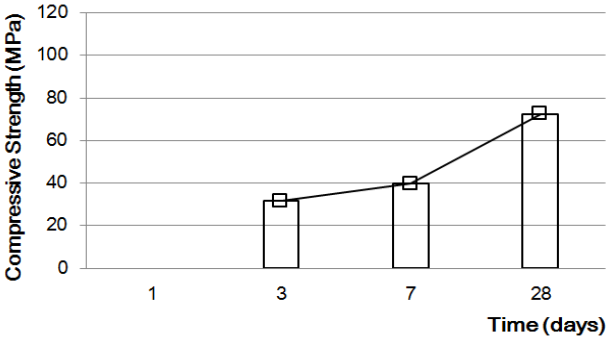

Figure 2: Compressive strength test results of Step 1

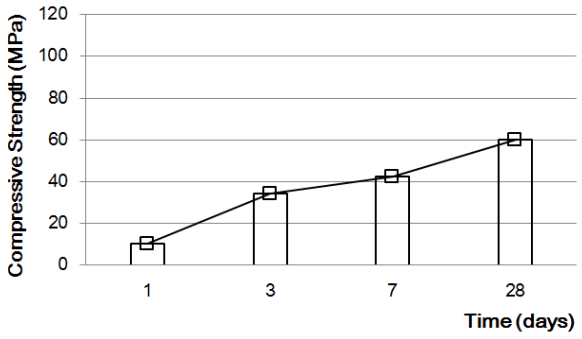

Figure 3: Compressive strength test results of Step 2

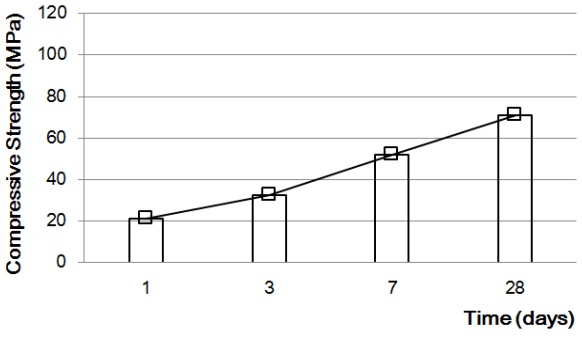

Figure 4: Compressive strength test results of Step 3

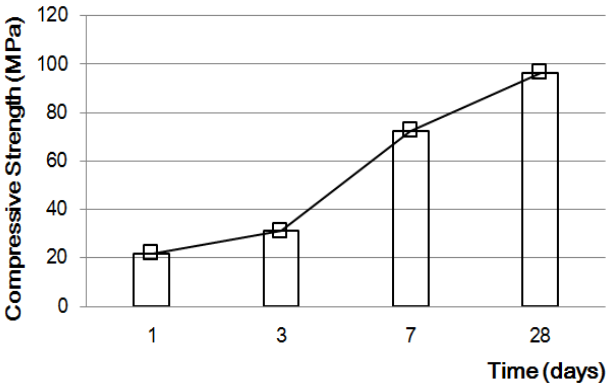

Figure 5: Compressive strength test results of Step 4

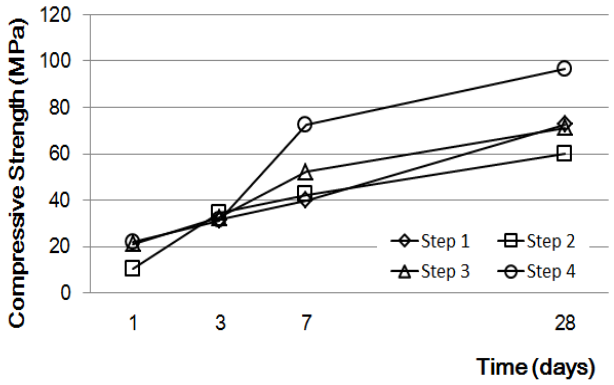

Figure 6: Compressive strength test results of all the steps

Stage 2-experiment results

Workability and density

In general, in the case of polymer cement mortar, KS F 2476 specifies that the flow must be 220 mm or more. The diameter of the test plate for measuring the flow was 300 mm. The flow was measured by performing 15 drop tests at a 12 mm drop height. Stage 1 showed the flow of 90–110 mm, which was significantly lower than the standard value. In the Stage 2 mix design, a retarding agent, antifoaming agent, and superplasticizer were used to improve the workability and the resulting flow met the target flow of 220 mm.

As the grout is injected by pumping, workability is an important factor. In Stage 2, the amount of superplasticizer was further increased and a floor value greater than 220 mm was obtained in the final mix with no material separation. Therefore, the Stage 2 design mix was judged as having excellent workability.

Table 10 shows the results of the density measurement.

The density of C.G.P was 23.4 kN/m^3 and that of D.G.P was 21.0 kN/m^3. Both satisfied the KS of 20 kN/m^3 or more.

Table 10: Density test results

Type (specification)	Specimen	Mass (g)	Cross-sectional area (mm^2)	Density (kN/m^3)
C.G.P (40x40) Commercial products	C-1	600.0	256	23.44
	C-2	601.7		23.50
	C-3	598.2		23.37
	AVG.	600.0		23.44
D.G.P (40x40) Developed products	D1	538.5	256	21.0
	D2	536.5		21.0
	D3	540.6		21.1
	AVG.	573.6		21.0

Strength properties

As shown in **Figure 7**, the compressive strength of D.G.P at 28 days of age was 102.6 MPa. The early strength at 1 day was 43.1 MPa, which was higher than the target value of 40 MPa. The elastic modulus of D.G.P calculated by equation (1) using the compressive strength was 40.6 MPa at 28 days of age, which was also higher than the target value of 40 GPa.

$$E_c = 8500\sqrt[3]{f_{ck}}$$

Equation (4)

$$E_c = \sqrt[3]{102.6 + 6} = 40{,}553\text{MPa} = 40.6\text{GPa}.$$

As shown in **Figure 8**, the flexural strength at 28 days was 14.4 MPa, which met the target performance. In the case of steel pipes and grout used for wind power generation, the problems of peeling off or lifting between different materials and separation due to thermal vibration/impact may occur after construction. In addition, they are subjected to tensile or compressive force generated by wind from the sea. If the inner grout separates from the steel pipes, it cannot cope with the external deformation due to internal slip. If different materials exhibit different behaviors, the strength is subject to a sharp decline. Therefore, in this study, the bond strengths of D.G.P and C.G.P were evaluated by attaching them to the existing concrete member. As a result, the bond strength and pullout-out strength of the D.G.P at 29 days of age were 1.7 kgf/cm^2 and 13.1 MPa, respectively, as shown in **Figure 9 and Table 11**. These values were higher than those of the C.G.P and satisfied the target performance.

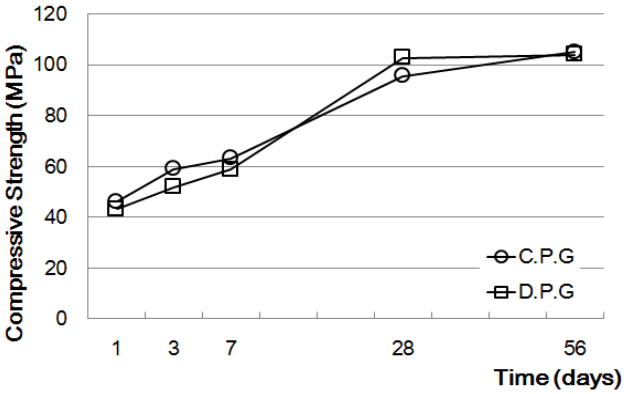

Figure 7: Compressive strength test results (C.G.P: Commercial grout products; D.G.P: Development grout products)

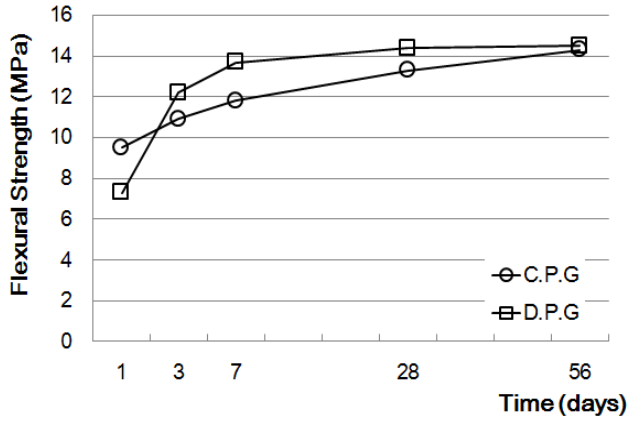

Figure 8: Test results for flexural strength

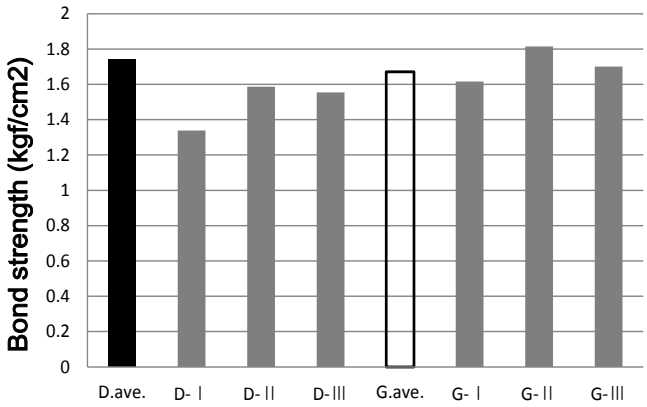

Figure 9: Test results for bond strength

Table 11: Test results for pullout strength

	Load (kN)	Embedment Length (mm)	Bar Diameter (mm)	Stress (MPa)
C.G.P 1	38.28	64	16	11.90
C.G.P 2	40.67	64	16	12.64
C.G.P 3	39.52	64	16	12.28
Aver.	39.49	64	16	12.28
D.G.P 1	42.50	64	16	13.21
D.G.P 2	42.70	64	16	13.27
D.G.P 3	41.20	64	16	12.81
Aver.	42.13	64	16	13.10

Durability properties

Figure 10 shows the measurement results for autogenous shrinkage within 24 h. In general, the ultra-high-strength grout has many advantages such as member cross section reduction, durability improvement, and weight reduction. However, there is a problem of autogenous shrinkage due to an increase in the cement amount per unit [17]. Such autogenous shrinkage occurs due to the self-drying of the capillary tube pores inside the concrete because of lack of external moisture supply. It mostly occurs in ultra-high-strength concrete with a low water-to-cement ratio and a high binder amount per unit, and may cause cracks. Such cracks provide a penetration path for harmful substances including chlorine ions, carbon dioxide, and moisture from the outside. This lowers the durability of the structure and shortens its life [18,19,20]**.**

The autogenous shrinkage of the D.G.P at 28 days of age was 276×10^{-6}. Although it was slightly higher than 80×10^{-6} of the C.G.P, it satisfied the target of 300×10^{-6}. For the samples of age less than 24 h, the results before 3 h showed no significant difference between the C.G.P and the D.G.P. However, after approximately 3 h, the C.G.P showed slight expansion whereas the C.G.P exhibited minute shrinkage. At 28 days after demolding, an autogenous shrinkage of approximately 80×10^{-6} occurred in the C.G.P. Likewise, an autogenous shrinkage of 450×10^{-6} occurred in the D.G.P. Furthermore, unlike the C.G.P in which autogenous shrinkage generally enters a phase of stagnation within 14 days, the D.G.P showed continuous shrinkage for 28 days.

Figure 11 shows the autogenous shrinkage results at 28 days of age. The D.G.P showed a higher autogenous shrinkage than the C.G.P. This result was higher than the existing result of 350×10^{-6}, indicating a need to reconsider the mix in the future. The investigations of the autogenous shrinkage characteristics of the C.G.P and D.G.P revealed that it is necessary to analyze the influence of the various factors on the shrinkage observed in the D.G.P through the analysis of the microstructures such as hydration. It is also necessary to consider measures to control shrinkage by using admixtures such as shrinkage reducing agents as well as ensuring appropriate curing before the application of the D.G.P to sites and structural members.

Atis et al. [21] argued that such long-term shrinkage could cause micro-cracks and reduce the structural strength. Therefore, it is necessary to carefully consider the long-term autogenous shrinkage of the D.G.P in the future.

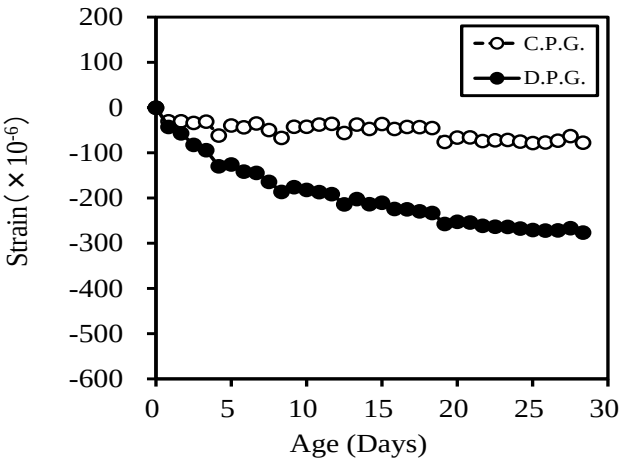

Figure 10: Test results for autogenous shrinkage (24 h)

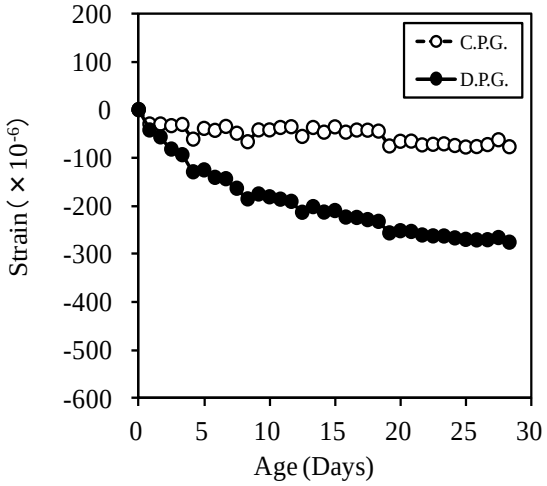

Figure 11: Test results for autogenous shrinkage (28 days)

Figure 12 shows the carbonation measurement results. Because of the accelerated carbonation test, excellent carbonation resistance characteristics were exhibited in the D.G.P compared to the C.G.P. In the C.G.P, a carbonation penetration depth of approximately 6.6 mm was measured at 1 week of age. On the other hand, the D.G.P exhibited a significantly different depth of 3.7 mm. Later, at 8 weeks of age, the C.G.P showed carbonation up to 16.3 mm, whereas the D.G.P exhibited carbonation of 11 mm, indicating a significant difference.

The carbonation depth of long-term aging was predicted through the application of the above results to the general carbonation model based on the $\sqrt{t}$ law. The carbonation coefficients of the C.G.P and the D.G.P were 3.0 and 4.7, respectively. Using these values, the carbonation depths after 16 weeks and after a decade were predicted as shown in **Figure 13**. It was assumed that the accelerated carbonation period of 16 weeks corresponded to the building use period of a decade. The C.G.P exhibited a 31.8 mm carbonation depth, which exceeded the generally used concrete cover thickness of 40 mm. In the case of the D.G.P, the carbonation depth was 31.8 mm and there was no corrosion damage on the reinforcing bars caused by carbonation. It was confirmed that the D.G.P exhibited better carbonation resistance performance than C.G.P.

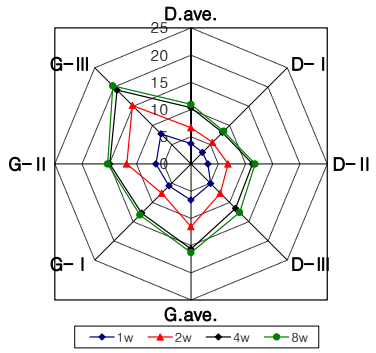

Figure 12: Accelerated carbonation test results

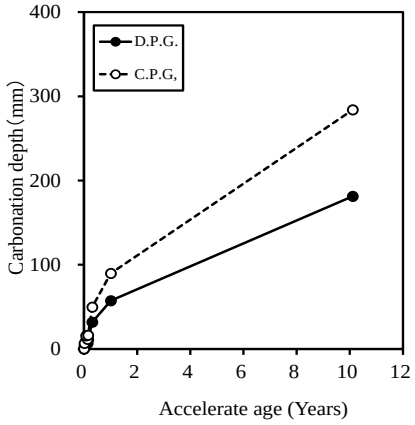

Figure 13: Accelerated carbonation prediction results

Figure 14 shows the measurement results of the relative dynamic modulus of elasticity after 100 cycles of freezing and thawing. The relative dynamic moduli of elasticity of the C.G.P and D.G.P were 93% and 94%, respectively, which confirmed excellent freeze-thaw resistance performances.

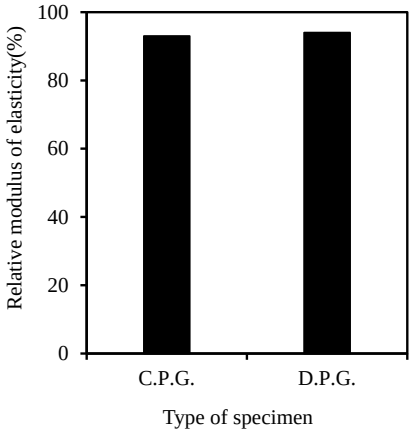

Figure 14: Test results for relative dynamic modulus of elasticity

Table 12 and Figure 15 show the chemical resistance measurement results. The clear difference in appearance between the C.G.P and the D.G.P was confirmed by naked-eye examination. In particular, the difference was largest when they were immersed in hydrochloric acid for 28 days. All the specimens showed discoloration on the 7th day of immersion. Gypsum generation was observed in the case of sulfuric acid immersion. In the case of D.G.P, the degradation (discoloration, gypsum generation, and disappearance and loss of surface layers) and mass reduction rates of the specimens were not observed significantly for all the chemicals (5% solutions of hydrochloric acid, sulfuric acid, and nitric acid). The mass reduction rate was not significantly different between the 7th day and 14th day of immersion.

The degradation caused by the acid component occurred at the beginning of immersion (0–7 days). After 14 days, however, the alkaline components rose to the surfaces of the specimens due to the hydration reactions inside those specimens, thereby increasing the pH of the immersion solutions. After 14 days of immersion, the pH of the immersion solutions remained constant because the hydration reactions inside the specimens were lowered. Therefore, the alkalinity of the surfaces of the specimens was lowered, which reduced the resistance to the acid and thus increased the mass reduction rate. After 28 days of immersion, the D.G.P showed 19% lower mass reduction than the C.G.P with hydrochloric acid, 1% with sulfuric acid, and 11% with nitric acid.

Table 12: Test results for chemical resistance

Division	Hydrochloric acid 5%			Sulfuric acid 5%			Nitric acid 5%		
	7th Day	14th Day	28th Day	7th Day	14th Day	28th Day	7th Day	14th Day	28th Day
C.G.P									
Weight ratio (%)	91	91	78	98	97	93	94	94	87
D.G.P									
Weight ratio (%)	98	98	97	99	98	94	98	98	98

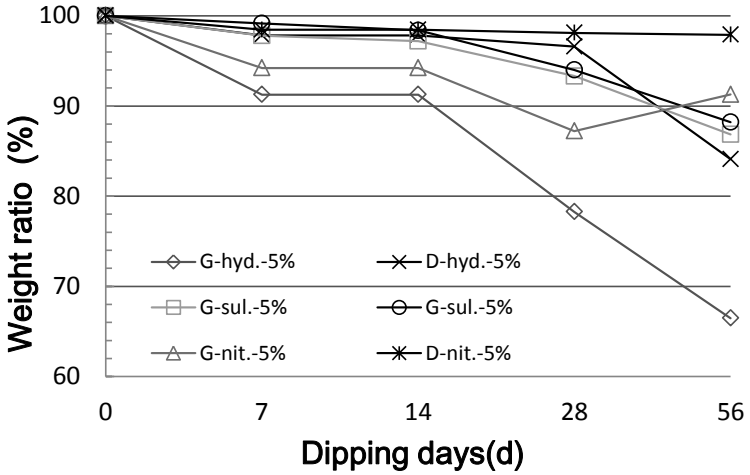

Figure 15: Test results for chemical resistance

CONCLUSION

In this study, ultra-high-strength grout was developed for filling steel pipes in offshore wind turbines and its workability, strength properties, and durability properties were evaluated.

Below are the results.

1. It was confirmed that the addition of the fine powders of silica fume and blast furnace slag for strength improvement was effective in early strength improvement but negatively affected the long-term strength improvement.
2. HSH-CSA and anhydrous gypsum were effectively used to improve the early strength; however, they negatively affected the long-term strength due to the formation of internal micro-cracks caused by the rapid increase of initial hydration levels. Therefore, it is necessary to carefully consider the usage ratio of the components.
3. The final mix of HSH-CSA and anhydrous gypsum (25%), silica fume (6.5%), and silica sand (40%) was

derived for the development of 100-MPa-class ultra-high-strength grout for offshore wind turbines, which was the objective of this study.

4. The test results of basic material properties such as early strength, modulus of elasticity, and density showed that all the intended goals of this study were satisfied.
5. With regard to chemical resistance, the developed grout showed lower mass reduction than the conventional grout by 19% with hydrochloric acid, 1% with sulfuric acid, and 11% with nitric acid based on the mass before immersion (100%). The developed grout also showed slow mass reduction during the immersion period.
6. The durability measurement results showed that the developed grout had higher durability than the conventional grout. The developed grout also exhibited higher bond and pullout strengths.
7. Based on the existing shrinkage specification of 350×10^{-6} or less, the conventional grout showed satisfactory results but the developed grout exceeded the range. Further studies are required to address the continued shrinkage of the developed grout after 7 days of immersion up to 28 days.

ACKNOWLEDGEMENT

This study was supported by a research fund from Songwon University

REFERENCES

[1] Environ Edinburgh, 2014, Hadyard Hill Extension Wind Farm, Environmental Impact Assessment (EIA) Scoping Report, SSE Renewables Developments (UK) Ltd.

[2] M.C. Han, R.F Song, Autogenous Shrinkage and Fundamental Properties of the High Strength Mortar Containing Waste Vegetable Oil, Korean Recycled Construction Resource Institute 5 (2010) 97–102.

[3] S.H. Oh, S.H. Hong, K.M. Lee, Autogenous Shrinkage Properties of High Strength Alkali Activated Slag Mortar, Journal of the Korean Recycled Construction Resources Institute 2 (2014) 60–65.

[4] X. Zhang, X. Zhou, H. Zhou, K. Gao, Z. Wang, Studies on forecasting of carbonation depth of slag high performance concrete considering gas permeability, Applied Clay Science 79 (2013) 36–40.

[5] G.S. Jang, H.D. Yun, S.W. Kim, W.S. Park, K.B. Choi, Flexural Behavior of Reinforced Concrete Beams Exposed to Freeze-Thawing Environments, Journal of the Korea institute for Structural Maintenance and Inspection 13 (2009) 126–134.

[6] Cheol Park, An Experimental Study on the Resistance to Surfuric Acid Attack in Concrete of Using Low Heat Blended Cement, Korea Concrete Institute (2013) 31–32.

[7] KS F 2476, Test method for polymer-modified mortar (2012).

[8] KS M 0602, Measuring methods for specific gravity of solid (2015).

[9] KS F 4042, Polymer modified cement mortar for maintenance in concrete structure (2012).

[10] KS F 2584, Standard test method for accelerated carbonation of concrete (2015).

[11] ASTM C 666-97, Standard Test Method for Resistance of Concrete to Rapid Freezing and Thawing.

[12] ASTM C 267-01, Standard Test Methods for Chemical Resistance of Mortars, Grouts, and Monolithic Surfacings and Polymer Concretes (Reapproved 2006).

[13] ASTM C 579-01 Standard Test Methods for Compressive Strength of Chemical-Resistant Mortars, Grouts, Monolithic Surfacings, and Polymer Concretes (Reapproved 2006).

[14] M.C. Han, R.F. Song, Autogenous Shrinkage and Fundamental Properties of the High Strength Mortar Containing Waste Vegetable Oil, Journal of the Korean recycled construction resources institute 5 (2010).

[15] X. Guo, H. Shi, W. Hu, K. Wu, Durability and microstructure of CSA cement-based materials from MSWI fly ash, Cement and Concrete Composites 46 (2014) 26–31. https://doi.org/10.1016/j.cemconcomp.2013.10.015

[16] G.M. Kim, J.G. Jang, H.R. Khalid, H.K. Lee, Water purification characteristics of pervious concrete fabricated with CSA cement and bottom ash aggregates, Construction and Building Materials 136 (2017) 1–8. https://doi.org/10.1016/j.conbuildmat.2017.01.020

[17] T. Ji, D.D. Zheng, X.F. Chen, X.J. Lin, H.C. Wu, Effect of prewetting degree of ceramsite on the early-age autogenous shrinkage of lightweight aggregate concrete, Construction and Building Materials 98 (2015) 102–111. https://doi.org/10.1016/j.conbuildmat.2015.08.102

[18] J.P. Won, S.H. Kim, S.J. Lee, S.J. Choi, Shrinkage and durability characteristics of eco-friendly fireproof high-strength concrete, Construction and

Building Materials 40 (2013) 753–762.
https://doi.org/10.1016/j.conbuildmat.2012.11.028

[19] E. Ghafari, S.A. Ghahari, H. Costa, E. Júlio, A. Portugal, L. Durães, Effect of supplementary cementitious materials on autogenous shrinkage of ultra-high performance concrete, Construction and Building Materials 127 (2016) 43–48.
https://doi.org/10.1016/j.conbuildmat.2016.09.123

[20] X. Hu, Z. Shi, C. Shi, Z. Wu, B. Tong, Z. Ou, G. de Schutter, Drying shrinkage and cracking resistance of concrete made with ternary cementitious components, Construction and Building Materials 149 (2017) 406–415.
https://doi.org/10.1016/j.conbuildmat.2017.05.113

[21] C.D. Atis, A. Kilic, U.K. Sevim, Strength and shrinkage properties of mortar containing a nonstandard high-calcium fly ash, Cement and Concrete Research 34 (2004) 99–102.
https://doi.org/10.1016/S0008-8846(03)00247-3